# A Three-Parameter One-Dimensional Model To Predict the Effectiveness Factor for an Arbitrary Pellet Shape

Clarisa Mocciaro,[†,‡] Néstor J. Mariani,[†,‡] Osvaldo M. Martínez,[†,‡] and Guillermo F. Barreto*[†,‡]

[†]PROIRQ , Departamento de Ingeniería Química, Facultad de Ingeniería, UNLP, La Plata, Argentina
[‡]Centro de Investigación y Desarrollo en Ciencias Aplicadas "Dr. J. J. Ronco" (CINDECA) CCT La Plata, CONICET- UNLP, calle 47 No. 257, CP B1900AJK, La Plata, Argentina

**ABSTRACT:** A novel one-dimensional (1D) model to account for the diffusion-reaction problem in catalytic pellets with arbitrary shape is proposed. The model includes three geometrical parameters, which are fitted by matching the behavior of the actual pellet at high and low Thiele moduli simultaneously. The formulation presented here for the diffusion-reaction problem with arbitrary pellet shapes and for the geometric 1D approximation is intended for covering a wide range of cases, concerning kinetics (including thermal effects), transport models, and variable catalytic activity. In this contribution, the effect of critical geometrical ratios that is observed in some pellet shapes is focused on testing the performance of the 1D model, assuming isothermal first-order kinetics. Remarkable precision (errors of <2%) was reached in all of the tested cases.

## 1. INTRODUCTION

Several aspects should be considered for the analysis and simulation of catalytic reactor units. Accounting for the intraparticle diffusion and reaction inside the catalytic pellet is usually a critical issue when dealing with real pellet shapes, because the fluxes of reactants and products occur along two spatial coordinates (two-dimensional, 2D) or three spatial coordinates (three-dimensional, 3D). The computational task is readily affordable when a single set of conditions is undertaken. However, for simulation of a catalytic reactor with a single reaction, such evaluations have to be performed thousands of times. In addition, for applications such as reactor optimization, the number of evaluations will increase by orders of magnitude. When dealing with practical cases in which a set of reactions occurs, the amount of numerical calculations is further increased. Thus, it is of paramount importance to avoid the use of 2D or 3D time-consuming computations.

Many years ago, Aris,[1] simultaneously with other researchers, presented a very simple approach to reduce 2D or 3D problems to a one-dimensional (1D) problem, showing that, at large values of the Thiele modulus, the effectiveness factor for a single reaction is not dependent on the pellet shape, but just on the ratio of pellet volume to external surface area: $l = V_p/S_p$, which is defined as the *characteristic length* or *characteristic diffusion length*. To perform approximate evaluations at low and intermediate values of the Thiele modulus, any pellet geometry satisfying the actual value of $l$ could be adopted, as a simple slab of half-thickness $l$. The expected precision with this approximation is ~20% for relatively simple kinetics.

A more-convenient 1D model was proposed by Datta and Leung.[2] For this model, identified here as the Generalized Cylinder (1D-GC) model, diffusion is supposed to occur along the length of a hypothetical body of variable cross section according to $(1 − x)^\sigma$, with $x$ being the dimensionless spatial coordinate. Values of the model parameter $\sigma$ (which is the shape factor) can be obtained by matching a shape property of the actual pellet.

Mariani et al.[3,4] proposed two different criteria to estimate the shape factor $\sigma$ by forcing the 1D-GC model to match the second-order term of a series expansion of the effectiveness factor of the actual pellet either at high Thiele moduli or at low Thiele moduli. For the purpose of identifying whether the high or low Thiele moduli criteria are used, the 1D-GC model will be denoted as 1D-GCΓ or 1D-GCγ, respectively. (The parameters Γ and γ characterize such second-order terms of the series at high and low Thiele moduli, respectively. Γ is strongly dependent on the pellet shape and, without any significant loss of accuracy, can be regarded as being independent of the kinetic expression.[4] On the other hand, γ is strictly a geometrical parameter.[3])

The 1D-GCγ model was evaluated for isothermal linear kinetics by Mariani et al.,[3] and the 1D-GCΓ model was evaluated by Mariani et al. for isothermal linear kinetics[5] and for normal nonlinear kinetics, like LHHW rate expressions[6] ("normal" refers to reaction rates that decrease as the limiting reactant is consumed). Overall, the deviations of the results of the 1D-GC model from the actual pellet effectiveness factor was less than ~3%. Many different pellet geometries were tried. In particular, a large set of commercially available pellet shapes were tested.[5] Generally, the 1D-GCγ model showed, on average, somewhat higher precision than the 1D-GCΓ model. However, the evaluation of parameter γ is more involved than that of parameter Γ. In summary, under the conditions tested in the above quoted works, the level of precision provided by the 1D-GC can be regarded as being quite satisfactory, even for the most stringent practical application.

Nonetheless, further conditions explored to assess the accuracy of the 1D-GC model have revealed that errors in the estimations of the effectiveness factor can rise well above the level found in the above-summarized studies. In this regard, new geometric and kinetics features were investigated. The type of geometrical aspects can be best described by an example. Among the shapes analyzed in the work of Mariani et al.,[5] a four-hole cylinder was considered, with relative geometric dimensions provided by a manufacturer. If the diameter of the holes is increased, leaving the remaining dimensions fixed, the ratio between the thickness of the walls separating the holes and the characteristic length $\ell$ becomes critically small. As a result, the pellet shows significantly different diffusion lengths and the only available geometrical parameter of the 1D-GC model becomes unable to capture the behavior of the actual pellet with precision. Of course, some others geometries also show similar effects, when the aspect ratios between their dimensions are changed. One common and practically relevant effect is simply introduced by modifying the length of any cylindrical pellet characterized by a given cross-sectional shape.

On the other hand, abnormal kinetics leading to effectiveness factors greater than unity were tried and the performance of the 1D-GC model deteriorates as the diffusion-reaction system shows high parametric sensitivity, in particular, with respect to geometrical details of the pellet.

In this context, the type of diffusion-reaction problem in a 3D catalytic pellet, for which series solutions for the effectiveness factor at low and high Thiele moduli are available, is first presented in Section 2 of this contribution. Section 3 presents the new 1D model approximation, which is called the variable-diffusivity model (1D-VD) and introduces three parameters for matching the leading terms of the series solutions of the actual pellet *simultaneously*. Section 4 covers the specific objective of this contribution, which is analyzing the performance of the 1D-VD model when applied to approximate the behavior of a significant number of pellet shapes, in general, and some pellet shapes that show critical aspect ratios, in particular.

We anticipate that the 1D-VD model guarantees remarkable precision, with errors of <2% in all the cases when isothermal linear kinetics are considered. The results from the use of the 1D-VD model, along with abnormal reaction kinetics, are also quite satisfactory and will be presented in a forthcoming communication; they are presently systematized in relation to the appearance of solutions involving multiple steady states. In addition, a criterion for the safe use of the simpler 1D-GC model is discussed in terms of the shape parameters $\gamma$ and $\Gamma$ of the actual 3D pellet.

## 2. PROBLEM STATEMENT AND BEHAVIOR AT LOW AND HIGH THIELE MODULI

The diffusion-reaction problem in a catalytic pellet of arbitrary geometry can be written in the following way for the key species A diffusing according to Fick's law with constant effective diffusivity ($D_A$) and isothermally undergoing a single irreversible catalytic reaction, depending on its molar concentration ($C_A$):

$$D_A \nabla^2(C_A) = a(\mathbf{x'}) \prod_A (C_A) \qquad \mathbf{x'} \in V_P \qquad (1a)$$

$$C_A = C_A^s \text{ (constant)} \qquad \mathbf{x'} \in S_P \qquad (1b)$$

where $\prod_A$ is the consumption rate of A, and $V_P$ and $S_P$ are the volume and external surface of the pellet, respectively. $\nabla^2$ stands

for the Laplacian operator. [Remark: In this paper, the symbol $V_P$ will stand for both the spatial domain corresponding to the catalyst and its volume; similarly, $S_P$ stands for the domain of the permeable external surface and its area.]

The catalytic activity $a$ may be dependent on the position vector ($\mathbf{x'}$) inside the pellet and is normalized according to

$$\frac{1}{V_P} \int_{V_P} a(\mathbf{x'}) \, dV = 1 \qquad (2)$$

It is assumed that the activity $a$ at any point on $S_P$ is nonzero but not necessarily uniform.

Equations 1a and 1b can be rendered dimensionless, using the characteristic length $\ell$ (which is defined as $\ell = V_P/S_P$ (for the spatial coordinates), and the values of $C_A^s$ and $\prod_A^s$ at the external surface, (i.e., $Y = C_A/C_A^s$ and $r(Y) = \prod_A / \prod_A^s$):

$$\nabla^{*2}(Y) = \Phi^2 a(\mathbf{x}) r(Y) \qquad \mathbf{x} \in V_P^* \qquad (3a)$$

$$Y = 1 \qquad \mathbf{x} \in S_P^* \qquad (3b)$$

where $V_P^*$, $S_P^*$, $\nabla^{*2}$, and $\mathbf{x}$ are the dimensionless pellet volume, external pellet surface, Laplacian operator, and position vector, respectively.

As usual, the Thiele modulus is defined as

$$\Phi = \ell \left( \frac{\prod_A^s}{C_A^s D_A} \right)^{1/2} \qquad (4)$$

The effectiveness factor is defined as

$$\eta = \frac{1}{V_P^*} \int_{V_P^*} a(\mathbf{x}) r(Y) \, dV^* \qquad (5)$$

Although the formulation in eqs 3a and 3b is based on the relatively simple problem expressed by eqs 1a, 1b, and 2, it is important to stress that a more general problem for a single reaction with a generic kinetic expression, depending on the concentration of any species in the mixture and on temperature, more-complex mass-transport models (e.g., the Dusty Gas Model for mass transport) can be cast in the same formal way as the formulation in eqs 3a and 3b, provided that the composition, temperature, and pressure are uniform over $S_P$. In addition, the pellet body shows isotropy and uniformity, with regard to the mass- and heat-transport intrinsic properties, and the heat of reaction can be assumed to be constant. These restrictions allow the expression of any of the molar fluxes of the species in the mixture and the heat flux in terms of one of them (e.g., the key reactant species A), and final relationships between molar concentrations and temperature with $C_A$ can be established.[7] In this general case, the meaning of variables $Y$ and $r(Y)$ in eqs 3a and 3b, and the definition of the Thiele modulus (eq 4), change, as a consequence of the reduction procedure, according to the details provided in refs 8 and 9.

Accordingly, the series expansions for the effectiveness factor described in the remainder of this section and the 1D models discussed in Section 3 also encompass the general problem just discussed.

The solution of eqs 3a and 3b at low Thiele modulus has been addressed in the literature (e.g., Aris[10]). A regular perturbation analysis can be carried out to expand $\eta$ (eq 5) in powers of $\Phi^2$:

$$\eta = 1 - r'(1) \gamma \Phi^2 + \left( r'(1)^2 + \frac{1}{2} r''(1) \right) \beta \Phi^4 \qquad (6)$$

2747

dx.doi.org/10.1021/ie101296d |*Ind. Eng. Chem. Res.* 2011, 50, 2746–2754

where $r'(1) = (dr/dY)_{Y=1}$, $r''(1) = (d^2r/dY^2)_{Y=1}$, and the parameters $\gamma$ and $\beta$ are expressed as

$$\gamma = \frac{\int_{V_p^*} aG \, dV^*}{V_p^*} \tag{7a}$$

$$\beta = \frac{\int_{V_p^*} aG^2 \, dV^*}{V_p^*} \tag{7b}$$

and $G$ is the solution of

$$\nabla^{*2} G = -a(\mathbf{x}) \text{ in } V_p^* \tag{8a}$$

$$G = 0 \text{ on } S_p^* \tag{8b}$$

The expression shown in eq 6 is a three-term truncated series with $\mathcal{O}\left(\Phi^6\right)$. Note that the auxiliary field $G$ is not dependent on kinetics; hence, the parameters $\gamma$ and $\beta$ are dependent only on the geometry (and the catalytic activity profile) of the pellet. The solution of the problem defined by eqs 8a and 8b (for $G$) should be determined only once for a given pellet shape. We have found the COMSOL Multiphysics simulation environment (numerical solution of differential equations by the finite-element method) to be very appropriate to this end. Instead, if only the evaluation of $\gamma$ is required, the use of the boundary element method is especially suitable, as described by Mariani et al.,[3] where some approximations and analytical results for simple geometries are also given.

Assuming that the external surface $S_p$ is composed of smooth regions (i.e., pieces with continuous curvature radii, separated by edges), Keegan et al.[8,9] developed a formulation for the problem described by eqs 3a and 3b that allows $\eta$ (eq 5) for high Thiele modulus to be expressed as a two-term truncated series to the power of $1/\Phi$:

$$\eta = \left(\frac{I_1}{\Phi}\right)\overline{a_s^{1/2}} - \left(\frac{I_2}{\Phi^2}\right)\Gamma \tag{9}$$

where

$$I(Y) = 2\int_0^Y r(Y_0) \, dY_0 \tag{10a}$$

$$I_1 = [I(1)]^{1/2} \tag{10b}$$

$$I_2 = \frac{1}{I_1}\int_0^1 [I(Y)]^{1/2} \, dY \tag{10c}$$

$$\overline{a_s^{1/2}} = S_p^{-1}\int_{S_p} a_s^{1/2} \, dS \tag{10d}$$

where $a_s$ is the local activity on the external pellet surface $S_p$.

The parameter $\Gamma$, which results from the formulation presented in Keegan et al.,[8,9] can be expressed as

$$\Gamma = \frac{\ell}{S_p}\left[\int_{S_p}(\mathcal{Y}_s + A_s) \, dS + \int_W \omega(\theta) \, dW\right] \tag{11}$$

where

$$A_s = -\frac{a_s'}{2a_s}$$

$$\mathcal{Y}_s = \frac{1}{R_a} + \frac{1}{R_b}$$

and

$$a_s' = \nabla a \cdot \mathbf{n}$$

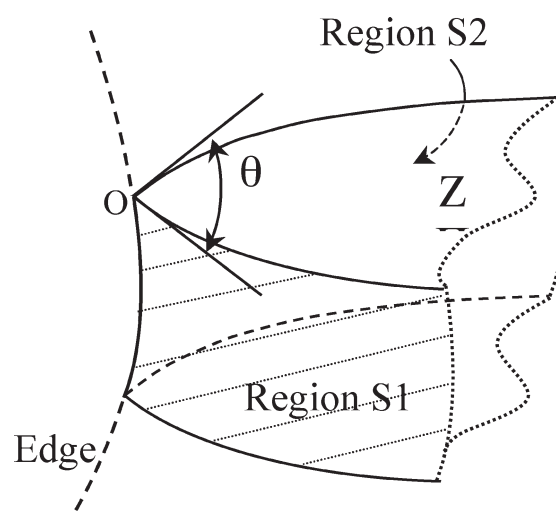Here, $\mathbf{n}$ is the inside normal unit vector on $S_p$.



**Figure 1.** Sketch showing the intersecting angle $\theta$.

$R_a$ and $R_b$ are the local principal radii of curvature on $S_p$, with the following sign convention: positive if the center of curvature is oriented toward the inside of the pellet and negative in the opposite sense. The variable $W$ in eq 11 accounts for the total length of the edges. Note that the definition of $\Gamma$ in eq 11 differs from the original given by Keegan et al.[9] by a factor $a_s^{1/2}$.

The coefficient $\omega$ is very weakly dependent on the type of reaction rate expression, but is strongly dependent on the *intersecting angle $\theta$* that a pair of smooth regions defines when they meet at the edge. The angle $\theta$ can be visualized in Figure 1, where the pair of smooth regions is denoted as region S1 and region S2. For curved regions, $\theta$ will generally vary with the position on the edge; in Figure 1, the angle $\theta$ corresponds to point O of the edge and Z is the plane normal to the edge at O.

The coefficient $\omega$ can be precisely evaluated from the following approximation:[9]

$$\omega(\theta) = \begin{cases} \dfrac{b_0}{\theta}\left[1 - \left(\dfrac{\theta}{\pi}\right)^{\pi^2/b_0}\right] & (\text{if } 0 \leq \theta \leq \pi) \\[2ex] \dfrac{\pi^2 A}{(\pi - A)\theta + \pi(2A - \pi)}\left(1 - \dfrac{\theta}{\pi}\right) & (\text{if } \pi < \theta \leq 2\pi) \end{cases} \tag{12}$$

where

$$b_0 = 5.2\left(\frac{I_1^{0.3}}{I_2^{0.1}}\right)$$

$$A = -\omega(2\pi) = \frac{1.9}{(I_1 I_2)^{0.07}}$$

Expression 11 for parameter $\Gamma$ looks complicated, because it has been written in a most general way. However, most commercially available pellet shapes show smooth regions with constant curvatures; hence, the integral on $S_p$ is very easily evaluated by adding the contribution of each region. Moreover, the edges normally present constant intersecting angles $\theta$ and the second integral also can be evaluated in a straightforward manner. The effect of kinetics on $\Gamma$ is introduced in eq 12 through parameters $I_1$ and $I_2$. However, this effect can be usually neglected by taking directly the values for isothermal linear kinetics, $r(Y) = Y$, $I_1 = 1$, and $I_2 = 1/2$.

In summary, the catalytic behavior of the actual pellet can be adequately characterized, at low and high Thiele modulus, by the shape parameters $\gamma$ (and $\beta$) and $\Gamma$, respectively.

## 3. ONE-DIMENSIONAL (1D) MODEL FORMULATION

For the purpose of approximating the diffusion-reaction process inside the actual pellet, a general 1D model is proposed, based on a hypothetical pellet allowing mass transport along only one spatial coordinate, $0 < x' < L$, where the origin is fixed at the external surface and $L$ is the diffusion length (this parameter will be specified later in this work). The dimensionless coordinate is defined as $x = x'/L$. For the 1D model to approximate the behavior of the actual pellet, it is necessary to introduce some fitting parameters. In a general way, these parameters can be associated with (fictitious) spatial variations of any of the following properties of the 1D model: cross-sectional area, catalytic activity, and effective diffusivity:

$$\text{Cross-sectional area :} \quad S_p A(x) \qquad A(0) = 1 \qquad (13a)$$

$$\text{Catalytic activity :} \quad (\overline{a_s^{1/2}})^2 a_m(x), \quad a_m(0) = 1 \qquad (13b)$$

$$\text{Diffusivity :} \quad D_A D^*(x), \quad D^*(0) = 1 \qquad (13c)$$

In eqs 13a, 13b, and 13c, the magnitudes $S_p$, $D_A$, and $\overline{a_s^{1/2}}$ (see eq 10d) correspond to the values for the actual pellet.

Therefore, the fictitious spatial-dependent coefficients are $A(x)$, $a_m(x)$, and $D^*(x)$. Their values at $x = 0$ have been fixed, for the sake of convenience; however, apart from this boundary restriction, they can vary arbitrarily with $x$, with the further condition of being positive, to keep their physical meaning. Trial functions for them should introduce the necessary fitting parameters. In practice, only one of them can be chosen as being effectively variable, relative to $x$, and the remaining two must be taken as constants (i.e., unitary). For example, the 1D-GC model becomes defined by using the expressions $D^*(x) = a_m(x) = 1$ and $A(x) = (1-x)^\sigma$.

We stress that the coefficient $a_m(x)$ is not intended to approximate the activity distribution $a(\mathbf{x})$ in the actual pellet (which, in fact, can be uniform). Seemingly, $D^*(x)$ will not reflect a true feature of the actual pellet (on the contrary, it has been stated in Section 2 that transport properties are restricted, to be intrinsically independent of position).

The dimensionless mass conservation balance for the key species A in the hypothetical pellet with the same dimensionless reaction rate $r(Y)$ and Thiele modulus $\Phi$ as in the actual pellet becomes

$$\frac{1}{A(x)} \frac{d}{dx}\left[A(x)D^*(x)\frac{dY}{dx}\right] = (\overline{a_s^{1/2}})^2 a_m(x)\left(\frac{L}{\ell}\right)^2 \Phi^2 r(Y) \qquad (14a)$$

$$Y = 1 \qquad \text{at } x = 0 \qquad (14b)$$

$$\frac{dY}{dx} = 0 \qquad \text{at } x = 1 \qquad (14c)$$

The effectiveness factor for the hypothetical pellet is

$$\eta = \frac{\int_0^1 a_m(x)A(x)r(Y)\, dx}{\int_0^1 a_m(x)A(x)\, dx} \qquad (15)$$

The first matching condition for the problem stated in eqs 14a, 14b, and 14c, and, to approximate that of the actual pellet (eqs 3a and 3b), is that both show the same global consumption rate at very low reaction rates ($\Phi \rightarrow 0$) (i.e., when the composition and temperature), and, hence, the reaction rates are uniform within the entire catalyst pellet. This condition allows $L$ to be defined and is expressed as

$$L = \frac{\ell}{(\overline{a_s^{1/2}})^2 \int_0^1 a_m(x)A(x)\, dx} \qquad (16)$$

The same global consumption rate in both pellets (hypothetical and actual) at very high $\Phi$ values (i.e., when only the first term is significant in eq 9) is automatically warranted by eqs 14a, 14b, and 14c and the conditions $A(0) = D^*(0) = a_m(0) = 1$ (see eqs 13a, 13b, and 13c).

The functions for $A(x)$, $D^*(x)$, and $a_m(x)$ can now be chosen to match further terms in the series shown in eqs 6 and 9 for both pellets. Clearly, as stated previously, we have identified only three shape parameters for the actual pellet ($\gamma$, $\beta$, $\Gamma$) and we have plenty of alternatives to introduce parameters in the three functions. To simplify matters, it was decided that only one coefficient would be used for this purpose and the remaining two would be assumed to be equal to unity. As a test for choosing the suitable function, it was assigned alternatively to each of them the form $f(x) = \exp(C_1 x + C_2 x^2)$, where $C_1$ and $C_2$ are parameters used to match the values $\gamma$ and $\Gamma$ of any actual pellet. The ability of each function to match simultaneously values of $\gamma$ and $\Gamma$, chosen independently, then was analyzed. The results were conclusive: the coefficient for diffusivity $D^*(x)$ is capable to adjust any combination of values with physical meaning (i.e., $\gamma > 0$ and $\Gamma > -1$), while $A(x)$ and $a_m(x)$ showed significant restrictions, because the range of values for $\gamma$ or $\Gamma$ was generally limited by the value taken for the other. Details of this test are given in Mocciaro's thesis.[11]

Therefore, we have chosen $D^*(x)$ and assumed a value of $A(x) = a_m(x) = 1$ in eq 14a. The specific model thus generated has been termed the *variable diffusion model* (denoted as 1D-VD). Equations 14−16 become

$$\frac{d}{dx}\left[D^*(x)\frac{dY}{dx}\right] = \frac{\Phi^2}{(\overline{a_s^{1/2}})^2} r(Y) \qquad (17a)$$

$$Y = 1 \qquad \text{at } x = 0 \qquad (17b)$$

$$\frac{dY}{dx} = 0 \qquad \text{at } x = 1 \qquad (17c)$$
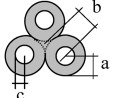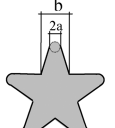
$$\eta = \int_0^1 r(Y)\, dx \qquad (18)$$

$$L = \frac{\ell}{(\overline{a_s^{1/2}})^2} \qquad (19)$$

The model represented by eqs 17a−c corresponds to a slab with uniform catalytic activity and an effective diffusivity that is dependent on position.

The following expression for $D^*(x)$, including three parameters, has been employed for the results discussed in the next section:

$$D^*(x) = \exp(C_1 x + C_2 x^n) \qquad (20)$$

**Table 1. Cross Section of Multilobe Pellets[a]**

| Pellet | Cross section | Dimensions | h | $\varepsilon_{max}$ (%) 1D-GC$\Gamma$ | $\varepsilon_{max}$ (%) 1D-VD |
|---|---|---|---|---|---|
| 8-lobes (8L) | | a=0.383 b | 0.657 | 1.5 | -0.4 |
| | | | 1 | 4.8 | 0.3 |
| Trilobe 3 hole ring (3L-3H) | | a=0.866 b c=0.5 a | 0.684 | 1.3 | 0.3 |
| | | | 1 | 3.0 | -0.4 |
| Star ring 1 | | a=0.292 b | 0.783 | 2.8 | 0.4 |
| | | | 1 | 5.3 | -0.3 |

[a] $h = H/(H + b)$.

where $C_1$, $C_2$, and $n$ are the constants to be fitted by matching the actual pellet shape parameters $\gamma$, $\beta$, and $\Gamma$. By expanding the effectiveness factor of the 1D-VD model (eq 18) in a series of $\Phi$ and $1/\Phi$ for low and high reaction rates, respectively, equations of the form shown in eqs 6 and 9 arise. From them, the following expressions can be obtained:

$$\Gamma = -\frac{1}{2}\left(\overline{a_s^{1/2}}\right)^2 \left(\frac{dD^*(x)}{dx}\right)_{x=0} \tag{21a}$$

$$\gamma = \frac{1}{\left(\overline{a_s^{1/2}}\right)^2}\int_0^1 \frac{(1-x)^2}{D^*(x)}\,dx \tag{21b}$$

$$\beta = \frac{1}{\left(\overline{a_s^{1/2}}\right)^4}\int_0^1 \mathscr{G}^2(x)\,dx \tag{21c}$$

where the function $\mathscr{G}(x)$ is defined as follows:

$$\mathscr{G}(x) = \int_0^x \frac{1-x}{D^*(x)}\,dx \tag{21d}$$

Note that $C_1$ is immediately obtained from eqs 20 and 21a: $C_1 = -2\Gamma/\left(\overline{a_s^{1/2}}\right)^2$. $C_2$ and $n$ can be obtained by solving numerically the pair of nonlinear simultaneous equations (eqs 21b and 21c), once the values of $\gamma$ and $\beta$ of the actual pellet are given. The constant $C_2$ may be positive or negative, whereas $n$ should be positive.

## 4. RESULTS

Since the specific purpose of this contribution is the analysis of the effect of the pellet shape on the estimation of the effectiveness factor using 1D models (1D-VD and the simpler 1D-GC), an isothermal first-order reaction and uniform catalytic activity for the actual pellet (i.e., $r(Y) = Y$ and $a = 1$ (and, hence, $a_s = 1$)) has been undertaken to this end.

A representative set of shapes, corresponding mostly to those of commercially available catalysts, has been considered. The shapes analyzed here, along with their standard relative dimensions, are defined in Tables 1 and 2, which include the relative error $\epsilon_{max}$ (defined in eq 22, given below) resulting from the effectiveness factor estimation when using the 1D-VD and 1D-GC$\Gamma$ models. All the pellets in Tables 1 and 2 are

cylinders of different cross-sectional shape, intended for a variety of chemical processes (oxidations, hydrogenations, isomerizations, hydrotreatments, steam reforming, etc.). The standard dimensions of the pellets reported in Tables 1 and 2 have been taken from manufacturers' catalogues (e.g., Haldor Topsoe, Criterion, BASF).

The relative errors in estimating the effectiveness factor ($\eta$) from 1D-VD and 1D-GC models are calculated from the following expression:

$$\epsilon = 100 \times \frac{\eta^m - \eta}{\eta}$$

where $\eta$ represents the effectiveness factor of an actual 3D pellet and $\eta^m$ represents the value obtained from the 1D-VD or 1D-GC.

According to the criteria employed to fit the parameters of both models, 1D-VD and 1D-GC, maximum errors (denoted by $\epsilon_{max}$) will take place for intermediate values of the Thiele modulus $\Phi$ (for the shapes described in Tables 1 and 2, the range of intermediate values was $0.5 < \Phi < 2$). Therefore, these maxima have been used to assess the behavior of both models:

$$\epsilon_{max} = \max_{\Phi}\{\epsilon\} \tag{22}$$

For a given 3D pellet, parameter $\Gamma$ was evaluated from eq 11, while parameters $\gamma$ and $\beta$ were obtained from eqs 7a and 7b after solving eqs 8a and 8b with the COMSOL Multiphysics environment. In addition, the effectiveness factor was obtained after solving the mass balance for the actual 3D pellet (eqs 3a and 3b) with the same software. Instead, a routine that was developed by the authors, which uses a shooting procedure to solve an integral formulation of the 1D conservation equations (see eqs 14a−c with $A(x) = (1 - x)^\sigma$, $D^*(x) = a_m(x) = 1$ for the 1D-GC model and eqs 17a−c for the 1D-VD model), was employed to obtain $\eta^m$. In either case, for the evaluation of $\eta$ or $\eta^m$, the size of the mesh for numerical evaluation was adjusted to guarantee an accuracy of ~0.1%.

With regard to the 1D-GC model, its parameter $\sigma$ was calculated either by matching the value $\gamma$ (for the 1D-GC$\gamma$ model) or $\Gamma$ (for the 1D-GC$\Gamma$ model) of the actual pellet, according to

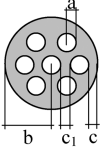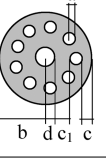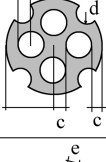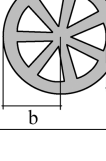$$\sigma = \frac{3\,\gamma - 1}{1 - \gamma} \tag{23a}$$

and
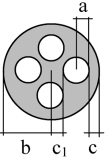
$$\sigma = \frac{\Gamma}{1 - \Gamma} \tag{23b}$$

As can be appreciated from Tables 1 and 2, the 1D-VD model allows a considerable reduction in the maximum error levels, up to a value of ~1% whereas, in the case of 1D-GC$\Gamma$ model, the maximum error is ~3% for the finite length cases. For the entire set of analyzed shapes, parameters of the 1D-VD model lay in the following ranges: $3 < n < 9$ and $0.35 < |C_2| < 9$, while we recall that $C_1 = -2\Gamma$ (for uniform catalytic activity in the actual pellet).

Results using the 1D-GC$\gamma$ model are not shown in Tables 1 and 2, because they are, on average, similar to those obtained using the 1D-GC$\Gamma$ model.

Recall that the geometrical ratios of the pellets in Tables 1 and 2 were taken from manufacturers' catalogs. However, some dimensions can show a distribution, as in the case of the pellet length, resulting from extrusion procedures. In addition, the same pellet shape frequently can be offered in more than a set of geometrical ratios, to seek specific advantages, either in catalyst

**Table 2. Cross Section of Multihole Pellets**[a]

| Pellet | Cross section | Dimensions | h | $\varepsilon_{max}$ (%) 1D-GC$\Gamma$ | $\varepsilon_{max}$ (%) 1D-VD |
|---|---|---|---|---|---|
| 4- hole ring (4H) |  | a=0.273 b  c=c$_1$=0.833a | 0.645 | 2.9 | -0.9 |
|  |  |  | 1 | 4.9 | -0.1 |
| 7-hole ring (7H) |  | a=1/2 b  c=c$_1$=a | 0.649 | 2.1 | 0.3 |
|  |  |  | 1 | 4.0 | 0.3 |
| 10-hole ring (10H) |  | a=1/8 b  c=1.6 a  c$_1$=2.4 a  d=2 a | 0.615 | 2.9 | 0.6 |
|  |  |  | 1 | 5.9 | 0.8 |
| Modified 4-hole ring (4HM) |  | a=1/4 b  c=a  d=0.831 a | 0.723 | 1.3 | 0.6 |
|  |  |  | 1 | 2.5 | 0.7 |
| 7-hole spoke ring (7SR) |  | e=0.2 b | 0.477 | 0.5 | 0.4 |
|  |  |  | 1 | 2.1 | -0.2 |

[a] $h = H/(H + b)$.

or reactor performance (e.g., increasing the diameter of the holes for a multihole pellet will lead to a decrease in reactor pressure drop and simultaneously may also lead to a higher effective reaction rate for strongly diffusion-limited conditions). Generally, such variations will be ultimately restrained by mechanical reasons,[12,13] because the structure of the pellet will be weakened by very thin internal walls or very sharp edges or points.

Therefore, addressing the performance of the 1D-VD and 1D-GC models when the geometrical ratios of the pellets are modified has been regarded to be a significant issue.

In this context, if we take into account the fact that the 1D-GC model is a simpler alternative, it would be interesting to know in advance when predictions of the 1D-GC start to deteriorate.

If the values of $\sigma$ calculated from both eqs 23a and 23b are similar, we can expect that the results of the 1D-GC model will be suitably precise. In the best case, both values of $\sigma$ from eqs 23a and 23b will be the same. Imposing this condition, the values of $\gamma$ and $\Gamma$ for the actual pellet would have to fulfill the following relation from eqs 23a and 23b:

$$1 = \gamma(3 - 2\Gamma)$$

In practice, however, for any actual pellet, we define the correlation parameter $C$ as

$$C = \gamma(3 - 2\Gamma) \quad (24)$$

Now, if the value of $C$ is close to 1, the 1D-GC model will be expected to be precise. Therefore, a convenient criterion for the safe use of the 1D-GC model can be formulated in terms of $C$. Figure 2 presents the values of $C$ for several shapes characterized by their values of $\Gamma$ and grouped by similarity, as multihole, multilobe, and miscellaneous shapes (this last set includes some shapes considered in Mariani et al.,[5] such as a hollow sphere, a torus, and other few cylindrical pellets with specific cross sections). Comparing the results of the actual effectiveness factors and those of the 1D-GC model for the set of pellets included in Figure 2, it has been concluded that $C$ should not deviate from unity by more than 15%, (i.e., 0.85 < C < 1.15, the region between the dashed lines in Figure 2) to keep the error of the 1D-GC model below 3% for an isothermal first-order reaction.

In the following sections, the effects of pellet length and cross-section relative dimensions will be analyzed for selected pellets of Tables 1 and 2.

**4.1. Effect of Pellet Length.** Note that when the length $H$ approaches zero ($H \rightarrow 0$), all pellets should behave as a slab, irrespective of the cross-sectional shape; in these cases, values of $\eta$ estimated by any of the 1D models considered here will be exact (i.e., with $\sigma = 0$ for the 1D-GC model and $D^*(x) \equiv 1$ for the 1D-VD model). The full effect of the cross section will manifest when $H \rightarrow \infty$. Therefore, the analysis that follows will be made for $0 < H < \infty$, or in terms of the dimensionless variable $h$, which is
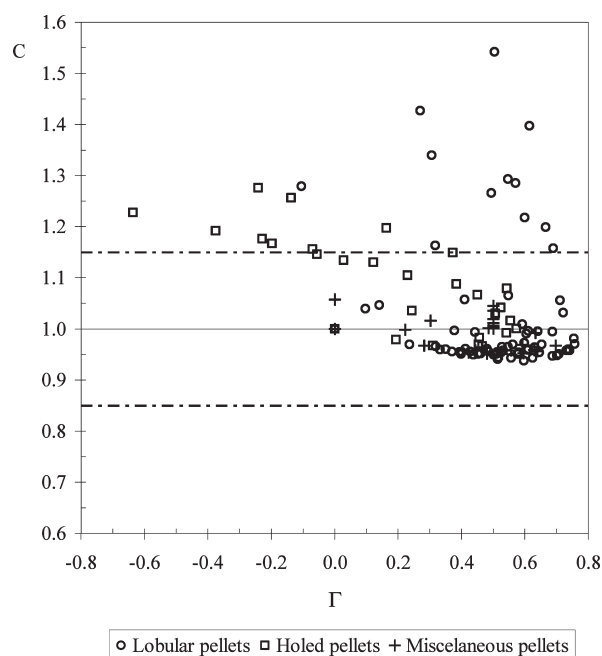
**Figure 2.** Values obtained for the correlation parameter $C$ for a collection of pellets characterized by $\Gamma$.

defined as $h = H/(H + b)$, $0 < h < 1$, where $b$ is a characteristic dimension of the cross section (see Tables 1 and 2).

Tables 1 and 2 also show the results of employing 1D-VD and 1D-GC$\Gamma$ models for infinitely long pellets ($h \rightarrow 1$), which is the most challenging case for all geometries in those tables. Interestingly, note that this condition is the one reached by a catalytic wall reactor in which a central channel is surrounded by a catalytic deposit of a given cross-sectional shape.

Figures 3a and 3b show the effect of pellet length on $\epsilon_{max}$ for two selected shapes from Tables 1 and 2 (8L (eight-lobe pellet) and 7H (seven-hole pellet), respectively). The $\epsilon_{max}$ value from the 1D-VD model clearly does not present any definite trend with $h$ and is bounded by 1%, whereas, for the 1D-GC model, $\epsilon_{max}$ increases monotonically and reaches the maximum value at an infinite length ($h = 1$): $\epsilon_{max} = 4.8\%$ and 4%, for the 8L pellet and 7H pellet, respectively.

The values of the correlation parameter in eq 24 at $h = 1$ are $C = 1.29$ for the 8L pellet and $C = 1.19$ for the 7H pellet. Both values of $C$ differ from the unity by more than 15% and, hence, do not fulfill the criterion for the safe use of the 1D-GC model. As could be expected, both values of $\epsilon_{max}$ are larger than 3%.

Note that the behavior shown in Figures 3a and 3b is typical for the entire set of shapes in Tables 1 and 2.

**4.2. Effect of the Pellet Cross-Sectional Parameters.** Three pellets from Tables 1 and 2 were selected to examine the effect of changing some geometrical ratios between their cross-sectional dimensions: star ring, 3L−3H (trilobe, 3-hole ring), and 4H (4-hole ring).

**4.2.1. Star Ring: Sharpness of the Star Points.** Figure 4 shows a sketch of the four star rings that will be analyzed. The difference is given by the $a/b$ ratio, which accounts for the curvature radius of the round point. The pellet identified as "star ring 1" is the one found in the manufacturer's catalog.

Table 3 shows the results for $h = 1$. It is evident that, as the star point becomes sharper (lower $a/b$ ratios), the errors using the 1D-GC model increase. In contrast, the 1D-VD model retains a very low error, without any appreciable trend.
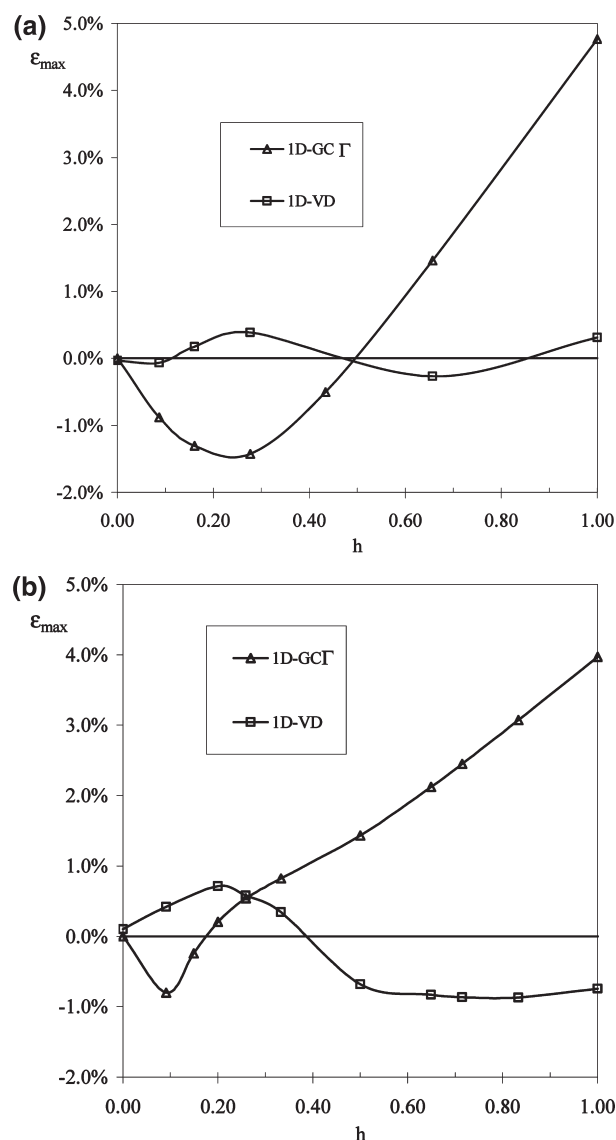


**(a)**



**(b)**

**Figure 3.** (a) Error in the 1D-GC-$\Gamma$ and 1D-VD models versus $h$ for (a) the 8L pellet and (b) the 7H pellet ($h = H/(H + b)$).



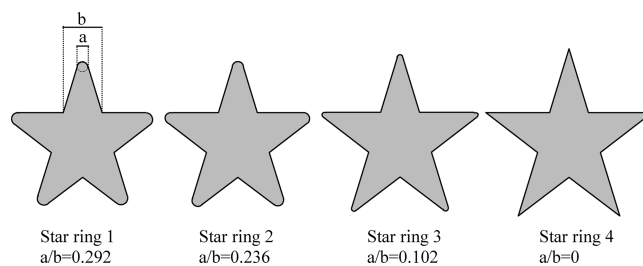| Star ring 1 | Star ring 2 | Star ring 3 | Star ring 4 |
| a/b=0.292 | a/b=0.236 | a/b=0.102 | a/b=0 |

**Figure 4.** Sketch for the cross section of the star ring pellets.

All values of $C$ in Table 3, except that for star ring 4, are well above 1.15 and, consequently, the values of $\epsilon_{max}$ for the 1D-GC model are >3%. The reason for this behavior is the small curvature radius of the round points, which define a region (tips of the points) with a diffusion length very different from that of the average in the entire pellet; then, the sharper the points, the greater the error. The particular behavior of star ring 4, with respect to the other three cases, is because the curved region at

**Table 3. Geometrical Parameters of the Four Star Rings and Maximum Errors, Using the 1D-GCΓ, 1D-GCγ, and 1D-VD Models[a]**

| pellet | $a/b$ | $\Gamma$ | $\gamma$ | $\beta$ | $C$ | $\epsilon_{max}$ (%) 1D-GCΓ | 1D-GCγ | 1D-VD |
|---|---|---|---|---|---|---|---|---|
| star ring 1 | 0.292 | 0.306 | 0.561 | 0.474 | 1.34 | 5.3 | −3.5 | −0.3 |
| star ring 2 | 0.236 | 0.270 | 0.580 | 0.521 | 1.43 | 6.4 | −4.1 | −0.2 |
| star ring 3 | 0.102 | 0.201 | 0.675 | 0.747 | 1.75 | 11.1 | −4.6 | −0.3 |
| star ring 4 | 0 | 0.774 | 0.818 | 1.116 | 1.19 | 2.8 | −1.0 | 0.5 |

[a] $h = H/(H + b) = 1$.



c = 0.75 a          c = 0.50 a          c = 0.25 a
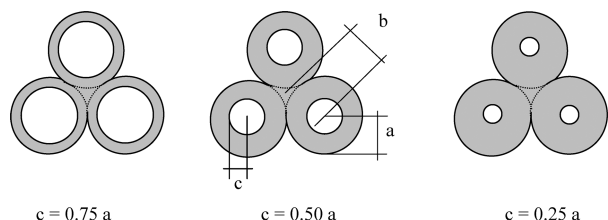
**Figure 5.** Sketch of the cross section of the trilobe pellets with three holes (3L−3H).

**Table 4. Geometrical Parameters and Maximum Errors, Using the 1D-GCΓ, 1D-GCγ, and 1D-VD Models for 3L-3H Pellets[a]**

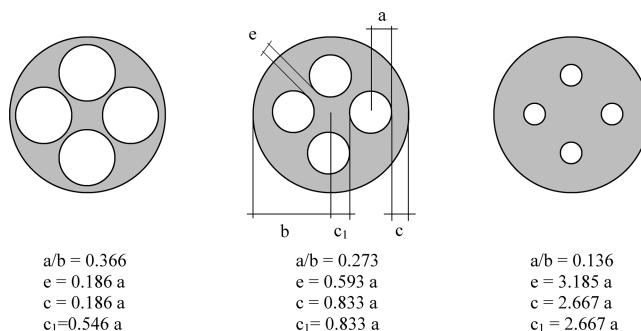| $h$ | $c/a$ | $\Gamma$ | $\gamma$ | $\beta$ | $C$ | $\epsilon_{max}$ (%) 1D-GCΓ | 1D-GCγ | 1D-VD |
|---|---|---|---|---|---|---|---|---|
| 0.684 | 0.75 | 0.200 | 0.551 | 0.747 | 1.43 | 2.8 | −8.0 | −0.8 |
| 0.684 | 0.50 | 0.318 | 0.492 | 0.421 | 1.16 | 1.3 | −3.8 | 0.3 |
| 0.684 | 0.25 | 0.383 | 0.485 | 0.349 | 1.08 | 0.8 | −1.8 | 0.7 |
| 1 | 0.75 | −0.044 | 0.504 | 0.627 | 1.56 | 4.1 | −9.8 | −1.1 |
| 1 | 0.50 | −0.105 | 0.399 | 0.270 | 1.28 | 3.0 | −5.7 | −0.4 |
| 1 | 0.25 | −0.197 | 0.351 | 0.170 | 1.19 | 2.4 | −3.3 | 0.3 |

[a] $h = H/(H + b)$.

the tip of the point becomes a perfectly defined edge, without the curvature effect of the others.

In practice, note that very sharp points would not be advisable because they most probably get broken when the catalyst is loaded into the reactor.

**4.2.2. Trilobe Pellet with Three Holes: Hole Diameter.** The geometrical parameter to be modified in the case of the trilobe pellet with three holes (3L−3H) is the diameter of the holes; simultaneously, the thickness of the separating wall between the internal and external surfaces changes, as shown in the three cases shown in Figure 5. In Table 4, the values of $\epsilon_{max}$ for the 1D-GC and 1D-VD models are reported at two different pellet lengths: $h = 0.684$ and $h = 1$. The 3L−3H pellet with ratios $c/a = 0.5$ and $h = 0.684$ corresponds to the commercial version.

Some points are worth remarking from the results in Table 4. On one hand, the 1D-VD model leads to errors considerably lower (less than ∼1%) than the 1D-GC model for almost all cases. Moreover, although the 1D-VD model does not present any trend with the $c/a$ ratio, for the 1D-GC model $\epsilon_{max}$ increases as the $c/a$ ratio decreases. Again, this fact clearly reflects the limitation of the 1D-GC model, because of the different effective diffusion length across the separating wall and the value for the



a/b = 0.366          a/b = 0.273          a/b = 0.136
e = 0.186 a          e = 0.593 a          e = 3.185 a
c = 0.186 a          c = 0.833 a          c = 2.667 a
$c_1$=0.546 a         $c_1$= 0.833 a        $c_1$ = 2.667 a

**Figure 6.** Sketch for the cross section of the four-hole ring pellets (4H).

**Table 5. Geometrical Parameters and Maximum Errors, Using the 1D-GCΓ, 1D-GCγ, and 1D-VD Models for the Analyzed 4H Pellets[a]**

| $h$ | $a/b$ | $c/a$ | $e/a$ | $l/a$ | $\Gamma$ | $\gamma$ | $C$ | $\epsilon_{max}$ (%) 1D-GCΓ | 1D-GCγ | 1D-VD |
|---|---|---|---|---|---|---|---|---|---|---|
| 0.645 | 0.367 | 0.186 | 0.186 | 0.233 | 0.122 | 0.658 | 1.81 | 11.2 | −6.4 | −1.4 |
| 0.645 | 0.273 | 0.833 | 0.593 | 0.520 | 0.164 | 0.448 | 1.20 | 2.9 | −3.3 | −0.9 |
| 0.645 | 0.136 | 2.667 | 3.185 | 1.652 | 0.146 | 0.422 | 1.14 | 2.5 | −2.0 | 0.7 |
| 1 | 0.367 | 0.186 | 0.186 | 0.257 | −0.12 | 0.600 | 1.94 | 14.0 | −7.3 | −1.6 |
| 1 | 0.273 | 0.833 | 0.593 | 0.616 | −0.24 | 0.366 | 1.28 | 4.9 | −4.4 | −0.1 |
| 1 | 0.136 | 2.667 | 3.185 | 2.196 | −0.58 | 0.299 | 1.24 | 6.1 | −3.1 | 0.6 |

[a] $h = H/(H + b)$.

entire pellet. The values of $C$ are also reported in Table 4. It can be observed that the criterion based on this correlation parameter is fulfilled.

As expected, the influence of the the $c/a$ ratio is more significant for an infinitely long pellet ($h = 1$).

**4.2.3. Four-Hole Ring: Hole Diameter.** In this case (4H pellet), the diameter of the holes is changed while keeping the external pellet diameter constant. Figure 6 shows the three cross sections resulting from decreasing the hole diameter by 50% and increasing the hole diameter by 35%, with respect to the standard case in Table 2 (4H pellet: $a/b = 0.273$ and $h = 0.645$).

Table 5 shows $\epsilon_{max}$ from employing the 1D-GC and 1D-VD models to estimate the effectiveness factor for the cases in Figure 6 and two different pellet lengths: $h = 0.645$ and $h = 1$.

$\epsilon_{max}$ grows well above 10% for $a/b = 0.367$ (the largest hole diameter, leading to the thinnest separating wall between holes) for both values of $h$. The corresponding values of the correlation parameter $C$ largely exceed the range previously suggested for confident use of the 1D-GC model.

It should be stressed that, for all pellets in Table 5, the 1D-VD model shows remarkable performance, with errors of ∼1%.

## 5. CONCLUSIONS

A novel one-dimensional (1D) model, called the *variable diffusion model* (denoted as 1D-VD), has been proposed to approximate the diffusion-reaction problem in actual three-dimensional (3D) catalytic pellets. The model can be described as a slab with uniform catalytic activity and a diffusion coefficient variable along the diffusion length, which introduces three constants that have been fitted by matching the behavior of the actual 3D pellet at high and low effective reaction rates simultaneously, as quantified by three shape parameters that are termed $\gamma$, $\beta$, and $\Gamma$.

For the objective of assessing the predictions of the 1D-VD model, values of the effectiveness factor were compared with those of the actual pellets and estimations from a previous one-parameter model, which is called the generalized cylinder model (denoted as 1D-GC), for a representative set of commercial pellets (standard case). A remarkable precision of ~1% was obtained by the 1D-VD model in the case of isothermal linear kinetics that has been studied in this contribution. These are encouraging results, especially bearing in mind that errors are expected to grow when dealing with abnormal nonlinear kinetics.

In addition, an analysis of the performance of the 1D-VD and 1D-GC models was undertaken when geometrical ratios of the pellets are modified from the standard case. The effect of pellet length was first addressed, while the influence of cross-sectional geometrical ratios was studied for some selected geometries (star ring, trilobe with three holes, and four-hole ring). In all cases, whereas large errors from the 1D-GC model are detected, the 1D-VD model allows for errors of ~1% to be retained.

In addition, a criterion based on the correlation parameter $C$ (readily calculated from the shape parameters $\gamma$ and $\Gamma$ of the actual 3D pellet) for safe use of the simpler 1D-GC model was analyzed.

## ■ AUTHOR INFORMATION

**Corresponding Author**
*E-mail: barreto@quimica.unlp.edu.ar.

## ■ ACKNOWLEDGMENT

## ■ NOMENCLATURE

$a(\mathbf{x})$ = local catalytic activity [-]
$A_s = -a_s'/(2a_s)$ [-]
$a_s$ = local catalytic activity on $S_p$ [-]
$A(x)$ = cross-section coefficient in the 1D-VD model [-]
$a_m(x)$ = coefficient for catalytic activity in the 1D-VD model [-]
$C_A$ = molar concentration of species A [mol m$^{-3}$]
$C_A^s$ = molar concentration of species A at the pellet surface [mol m$^{-3}$]
$D_A$ = effective diffusivity of species A [m$^2$ s$^{-1}$]
$D^*(x)$ = coefficient for the effective diffusivity in the 1D-VD model [-]
$G$ = auxiliary field defined in eqs 8a and 8b [-]
$\mathscr{G}$ = auxiliary field defined in eq 21d for the 1D-VD model [-]
$H$ = length of a cylindrical pellet [m]
$I_1$ = coefficient defined in eq 10b [-]
$I_2$ = coefficient defined in eq 10c [-]
$\ell$ = characteristic length; $\ell = V_p/S_p$ [m]
$L$ = diffusion length in the general 1D model [m]
$R$ = radial coordinate [m]
$r(Y)$ = dimensionless reaction rate; $r(Y) = \prod_A(Y)/\prod_A^s$ [-]
$R_a, R_b$ = principal radii of curvature [m]
$S_p^*$ = dimensionless pellet external surface accessible to reactants [-]
$V_p^*$ = dimensionless pellet volume [-]

$S_p$ = external surface area of the pellet accessible to reactants [m$^2$]
$V_p$ = pellet volume [m$^3$]
$W$ = total length of the edges [m]
$Y$ = dimensionless concentration [-]
$x$ = dimensionless coordinate in the 1D-VD model [-]
$x$ = dimensionless position vector inside the actual pellet [-]

**Greek Letters**

$\theta$ = intersecting angle at the edge (see Figure 1) [rad]
$\omega(\theta)$ = parameter related to the edges (see eqs 11 and 12) [-]
$\Pi_A$ = consumption rate of A [mol m$^{-3}$ s$^{-1}$]
$\Pi_A^s$ = consumption rate of A at the pellet surface [mol m$^{-3}$ s$^{-1}$]
$\beta$ = coefficient defined in eq 7b [-]
$\Phi$ = Thiele modulus [-]
$\Gamma$ = coefficient defined in eq 11 [-]
$\gamma$ = coefficient defined in eq 7a
$\eta$ = effectiveness factor [-]
$\sigma$ = shape factor, 1D-GC model parameter [-]
$\mathscr{Y}_s$ = sum of local principal curvatures on $S_p$; $\mathscr{Y}_s = (1/R_a) + (1/R_b)$ [m$^{-1}$]

**Superscripts and Subscripts**

s = value at $S_p$

## ■ REFERENCES

(1) Aris, R. A Normalization for the Thiele Modulus. *Ind. Eng. Chem. Fundam.* **1965**, *4*, 227–229.

(2) Datta, R.; Leung, S. W. K. Shape generalized isothermal effectiveness factor for first-order kinetics. *Chem. Eng. Commun.* **1985**, *39* (1), 155–173.

(3) Mariani, N. J.; Keegan, S. D.; Martínez, O. M.; Barreto, G. F. A one-dimensional equivalent model to evaluate overall reaction rates in catalytic pellets. *Chem Eng. Res. Des., Part A* **2003**, *81*, 1033–1042.

(4) Mariani, N. J.; Keegan, S. D.; Martínez, O. M.; Barreto, G. F. On the evaluation of effective reaction rates on commercial catalyst by means of a one-dimensional model. *Catal. Today* **2008**, *133−135*, 770–774.

(5) Mariani, N. J.; Mocciaro, C.; Keegan, S. D.; Martínez, O. M.; Barreto, G. F. Evaluating the effectiveness factor from a 1D approximation fitted at high Thiele modulus: Spanning commercial pellet shapes with linear kinetics. *Chem. Eng. Sci.* **2009**, *64* (11), 2762–2766.

(6) Mariani, N. J.; Mocciaro, C.; Keegan, S. D.; Martínez, O. M.; Barreto, G. F. Estimation of effectiveness factor for arbitrary particle shape and non-linear kinetics. *Ind. Eng. Chem. Res.* **2009**, *48* (3), 1172–1177.

(7) Stewart, W. E. Invariant solutions for steady diffusion and reaction in permeable catalysts. *Chem. Eng. Sci.* **1978**, *33*, 547–553.

(8) Keegan, S. D.; Mariani, N. J.; Martínez, O. M.; Barreto, G. F. Behavior of smooth catalyst at high reaction rates. *Chem. Eng. J.* **2005**, *110*, 41–56.

(9) Keegan, S. D.; Mariani, N. J.; Martínez, O. M.; Barreto, G. F. Behavior of catalytic pellets at high reaction rates. The effect of the edges. *Ind. Eng. Chem. Res.* **2006**, *45*, 85–97.

(10) Aris, R. *The Mathematical Theory of Diffusion and Reaction in Permeable Catalysts*; Oxford University Press: London, 1975.

(11) Mocciaro, C. Doctoral Thesis, *Fenómenos de Transporte En Reactores Trickle-Bed*, Universidad Nacional de La Plata, Argentina, 2010.

(12) Wu, D.; Zhou, J.; Li, Y. Mechanical strength of solid catalysts: Recent developments and future prospects. *AIChE J.* **2007**, *53* (10), 2618–2629.

(13) Li, Y.; Wu, D.; Zhang, J.; Chang, L.; Wu, D.; Fang, Z.; Shi, Y. Measurement and statistics of single pellet mechanical strength of differently shaped catalysts. *Powder Technol.* **2000**, *113*, 176–184.

2754

dx.doi.org/10.1021/ie101296d |*Ind. Eng. Chem. Res.* 2011, 50, 2746–2754